Coherent Atom-Phonon Interaction through Mode Field Coupling in Hybrid Optomechanical Systems

Michele Cotrufo* and Andrea Fiore
Department of Applied Physics, Eindhoven University of Technology, 5600 MB Eindhoven, The Netherlands

Ewold Verhagen
Center for Nanophotonics, AMOLF, Science Park 104, 1098 XG Amsterdam, The Netherlands
(Received 13 October 2016; published 30 March 2017)

We propose a novel type of optomechanical coupling which enables a tripartite interaction between a quantum emitter, an optical mode, and a macroscopic mechanical oscillator. The interaction uses a mechanism we term *mode field coupling*: a mechanical displacement modifies the spatial distribution of the optical mode field, which, in turn, modulates the emitter-photon coupling rate. In properly designed multimode optomechanical systems, we can achieve situations in which mode field coupling is the only possible interaction pathway for the system. This enables, for example, swapping of a single excitation between emitter and phonon, creation of nonclassical states of motion, and mechanical ground-state cooling in the bad-cavity regime. Importantly, the emitter-phonon coupling rate can be enhanced through an optical drive field, allowing active control of the emitter-phonon coupling for realistic experimental parameters.

DOI: 10.1103/PhysRevLett.118.133603

Interfacing different quantum systems, such as atoms, photons, and phonons, is a key requirement for quantum information processing. The well-established framework of cavity quantum electrodynamics (CQED) interfaces photons—ideal for communication—to natural or artifical atoms (quantum emitters, QEs), whose strong nonlinearities enable quantum processing. Mechanical resonators have recently come to the forefront due to their large coherence times and their interaction with photons in cavity optomechanical systems [1]. Moreover, creating nonclassical states in macroscopic mechanical systems is appealing for fundamental studies of quantum physics [2,3]. In these contexts, establishing an efficient and controllable interaction between phonons and QEs would be highly beneficial as it would enable using the QE nonlinearity for the creation and manipulation of phononic quantum states [4].

Different approaches have been proposed to realize such an interaction. First, a phonon can directly couple to a solid-state QE through mechanical strain [5–8]. Large coupling rates can be obtained in specific systems, but this effect is difficult to engineer and to dynamically control. A second approach couples mechanical modes dispersively to an optical cavity, which, in turn, interacts with a QE [9–12]. Tripartite entanglement and atom-assisted optomechanical cooling are predicted in the so-far-elusive regimes when the optomechanical interaction is nonlinear at the quantum level [9] or when the emitter-field coupling rate approaches the emitter frequency [11]. Additionally, a QE-phonon interaction occurs in molecules and solids when the electronic and vibrational degrees of freedom are coupled, leading to inelastic scattering processes. Natural Raman transitions have been used to transfer a photon's quantum state to an optical phonon in diamond [13,14], but the extremely high frequency and large dissipation limit general applications for quantum processing.

In this Letter, we propose a novel optomechanical effect that provides an explicit, engineerable, and optically controllable interaction between a QE and a macroscopic mechanical oscillator. The interaction arises from a mechanically induced modification of the spatial distribution of the optical field [Fig. 1(a)], which, in turn, modulates the QE-photon coupling rate. We show that this interaction is particularly strong in systems of weakly interacting optical cavities because the field variation, upon a perturbation, scales inversely with the frequency spacing between optical modes. In such systems, the combined effect of different bipartite interactions gives rise to a novel QE-photon-phonon coupling that we term *mode field coupling* (MFC). We show that MFC can become the only allowed interaction, enabling, e.g., QE-phonon excitation swapping and mechanical ground-state cooling in the bad-cavity regime. Importantly, the interaction can be controlled and enhanced by the optical field intensity, resulting in optically controlled emitter-phonon coherent manipulation. This coupling, and the resulting Hamiltonian, share important traits with Raman-like processes in trapped ions [15], which have proven powerful in controlling the motional state of single ions. MFC has, however, two distinct features: it involves large-mass macroscopic resonators, and its rate is nonetheless large enough to overcome the large decoherence typical of solid-state QEs.

Model.—We consider a standard CQED setup, in which a two-level QE couples to an optical cavity mode through the Hamiltonian $\hat{H} = \omega_A \hat{\sigma}_z/2 + \omega_c \hat{a}^\dagger \hat{a} + g(\hat{a}\hat{\sigma}_+ + \hat{a}^\dagger \hat{\sigma}_-)$,

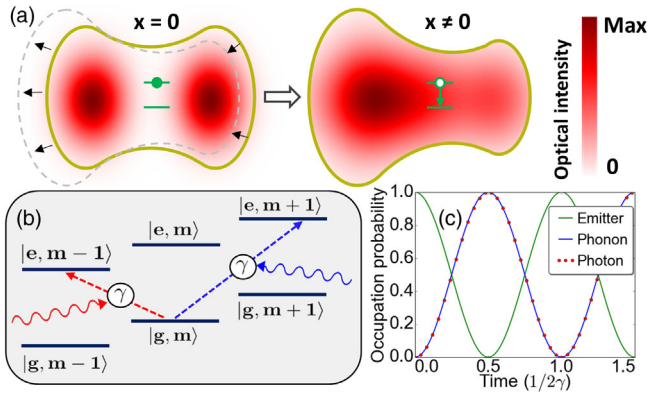

FIG. 1. (a) Sketch of the proposed concept. An optical cavity (yellow solid line) defines an electric field (red pattern), which is initially (left) zero at the QE position (green symbol). Upon boundary displacement (right), the field seen by the QE becomes nonzero and radiative transitions can occur. (b) Phonon-nonconserving transitions achievable through MFC. A photon red detuned (blue detuned) by Ω_M with respect to the QE stimulates transitions from $|g,m\rangle$ to $|e,m-1\rangle$ ($|e,m+1\rangle$). (c) Time evolution dictated by the Hamiltonian in Eq. (1), with the QE initially excited and $\omega_c = \omega_A - \Omega_M$.

where ω_A (ω_c) denotes the QE (optical) frequency, $\hat{a}$ is the photon annihilation operator, $\hat{\sigma}_{\pm,z}$ are Pauli operators describing the QE, and $\hbar = 1$. We initially neglect any loss, focusing on conservative interactions. The QE-photon coupling rate $g = -\mathbf{d}\cdot\mathcal{E}_0$ is determined by the emitter's transition dipole moment $\mathbf{d}$ and the electric field per photon $\mathcal{E}_0$ of the optical mode at the emitter position. Next, we consider a mechanical oscillator with frequency Ω_M and phonon annihilation operator $\hat{b}$. In a standard dispersively coupled optomechanical system, the resonator's displacement $\hat{x} = x_{\mathrm{zpf}}(\hat{b} + \hat{b}^\dagger)$ affects the cavity frequency. This interaction is quantified by the coupling rate $g_0 = -(\partial\omega_c/\partial x)x_{\mathrm{zpf}}$, where x_{zpf} is the zero-point motion amplitude. Here, we consider a fundamentally different situation in which the mechanical displacement induces a variation of the spatial distribution of the cavity field [Fig. 1(a)], while ω_c is negligibly affected. As a direct consequence, the emitter-cavity coupling rate g becomes dependent on the mechanical position. Up to first order in $\hat{x}$, $g(\hat{x}) = g(0) + \gamma(\hat{b} + \hat{b}^\dagger)$, where we defined the MFC coupling rate $\gamma = (\partial g/\partial x)|_{x=0}x_{\mathrm{zpf}}$. Inserting this expression in the Hamiltonian leads to the appearance of a tripartite interaction between the QE, optical field, and mechanical resonator. In the specific case that at mechanical equilibrium the field at the emitter's position vanishes [Fig. 1(a)], $g(0) = 0$, and the only possible interaction channel is the tripartite one. The interaction Hamiltonian reads

$$\hat{H}_{\mathrm{int}} = \gamma(\hat{b} + \hat{b}^\dagger)(\hat{a}\hat{\sigma}_+ + \hat{a}^\dagger\sigma_-). \tag{1}$$

This Hamiltonian allows swapping the excitation between the three quantum systems under particular resonant conditions. For $\omega_c \approx \omega_A + \Omega_M$ ($\omega_c \approx \omega_A - \Omega_M$), the dominant term is $\hat{b}^\dagger\hat{\sigma}_+\hat{a} + \mathrm{H.c.}$ ($\hat{b}\hat{\sigma}_+\hat{a} + \mathrm{H.c.}$), describing phonon and QE excitation upon photon annihilation (QE excitation due to photon and phonon annihilation) and the reverse process. Depending on the photon energy, therefore, the transitions $|g,m\rangle \leftrightarrow |e,m\pm1\rangle$ are realized [Fig. 1(b)], where e (g) denotes the QE excited (ground) state and m the phonon number. Figure 1(c) shows the lossless time evolution described by Eq. (1) for $\omega_c = \omega_A - \Omega_M$, with only the QE initially excited. The excitation oscillates at a frequency 2γ between the QE and the state formed by one photon and one phonon. Next, we consider pumping the cavity with a large coherent field to an average photon number n_{cav}, writing the cavity field as $\hat{a} = \sqrt{n_{\mathrm{cav}}} + \delta\hat{a}$. Neglecting for now the fluctuations $\delta\hat{a}$ (valid for $n_{\mathrm{cav}} \gg 1$), the Hamiltonian reads

$$\hat{H}_{\mathrm{int}} = \gamma\sqrt{n_{\mathrm{cav}}}(\hat{b} + \hat{b}^\dagger)(\hat{\sigma}_+ + \sigma_-), \tag{2}$$

which describes a coherent QE-phonon interaction, with a coupling rate controlled by n_{cav}. Thus, the optical intensity can enhance the QE-phonon coupling and, in particular, overcome system losses.

Creating large field variations.—We will now show that the effective MFC interaction Hamiltonian [Eq. (1)] can emerge from standard radiation-pressure forces in coupled-cavity systems. As the mode field is the solution of an eigenvalue problem [16], we look for a mechanical perturbation that induces strong changes of the eigenvector without affecting the eigenvalue. This is maximized for quasidegenerate unperturbed eigenvalues, which can be obtained by coupling multiple cavities such that hybridized modes ("supermodes") with well-defined symmetry are formed. Near a symmetry point, i.e., an anticrossing, an odd perturbation breaks symmetry. This localizes the supermodes in one of the cavities, resulting in a large variation of the local mode field.

Indeed, we find an example of MFC [Fig. 2(a)] in two identical optical cavities coupled with rate J (a *membrane-in-the-middle* setup [17,18]). A mechanical displacement that induces opposite detuning $\pm\Delta$ to each cavity affects the spatial distribution of the supermode amplitudes, and thereby their coupling rate ($g^{(\pm)}$) with an emitter placed in one cavity [Fig. 2(c)]. For $\Delta/J \ll 1$, the supermode frequencies are constant [Fig. 2(b)]; i.e., dispersive coupling is absent. Importantly, the MFC coupling rate γ is enhanced for weak intercavity coupling as it scales with J^{-1} (see Supplemental Material [19]): for weakly interacting cavities ($J \to 0$), small deviations from the condition $\Delta = 0$ quickly lead to localization of the supermodes into the individual cavities. In the two-cavity system, however, the tripartite MFC interaction competes with the Rabi emitter-photon interaction as $g^{(\pm)}(0) \neq 0$ [Fig. 2(c)].

This direct QE-photon interaction can be suppressed by introducing an additional optical cavity with identical frequency [Fig. 2(d)]. The middle cavity (T), containing the QE, interacts with both lateral cavities with rate J, leading to the formation of three supermodes $\hat{a}_+$, $\hat{a}_-$, and $\hat{a}_0$ [26,27]. For zero detuning, the mode $\hat{a}_0$ has opposite fields in the lateral cavities and zero field in T [blue line in

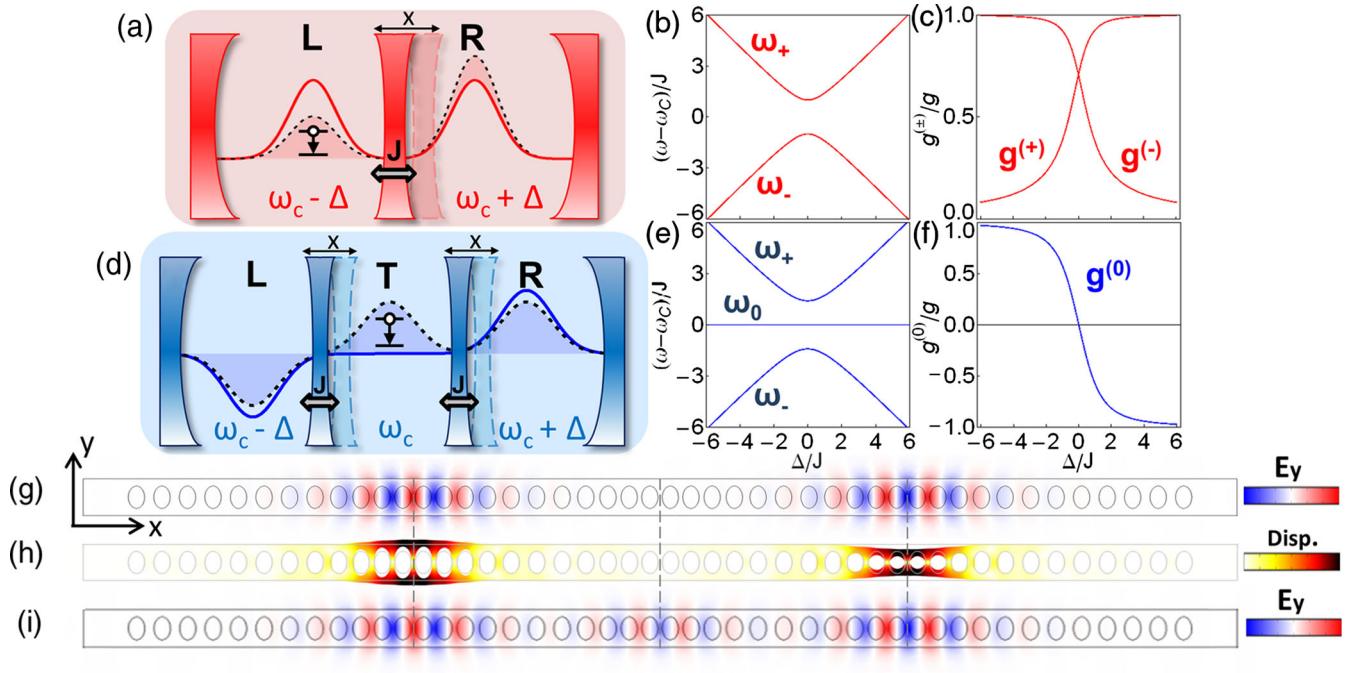

FIG. 2. (a) Two identical cavities interact at rate J through a partly transparent movable mirror. The symmetric optical supermode is sketched for zero detuning (red line) and equal and opposite detuning $\pm\Delta$ on the cavities (black dashed line). (b) Supermode frequencies versus Δ/J. (c) Coupling rates between a QE located in the left cavity (L) and the two supermodes (normalized to the coupling rate g with the uncoupled mode in L) versus Δ/J. (d) Three-cavity system. The field of the supermode of interest ($\hat{a}_0$) is shown as a blue (black dashed) line for zero ($\pm\Delta$) detuning of the lateral cavities. (e) Supermode frequencies in the three-cavity system. (f) Normalized coupling rate between a QE located in cavity T and the supermode $\hat{a}_0$. (g)–(i) Implementation based on three defect cavities in a photonic crystal nanobeam. Vertical dashed lines mark cavity positions. (g) Electric field (y component) of $\hat{a}_0$ at mechanical equilibrium. (h) Displacement pattern of the selected mechanical mode. (i) Expected field of $\hat{a}_0$ upon mechanically induced perturbation ($\Delta/J = 0.5$). Additional details in [19].

Fig. 2(d)], and therefore, does not interact with the QE. We now consider a mechanical mode that detunes only the frequencies of the lateral cavities by $\pm\Delta$, while leaving T unperturbed. This could be realized for example by rigidly connecting the two membranes. More generally, it can be obtained by dispersively coupling each optical cavity at a rate g_0 to a separate mechanical oscillator [19]. If these three identical oscillators are coupled mechanically, one resulting mechanical supermode has equal and opposite dispersive interaction with the lateral cavities with a rate $\pm g_0/\sqrt{2}$ and zero interaction with T. The frequency of $\hat{a}_0$ is unaltered by such detuning [Fig. 2(e)], while its field in T becomes finite [Fig. 2(d), dashed line], which translates in a large modulation of the coupling rate $g^{(0)}$ between $\hat{a}_0$ and the QE around the value $g^{(0)} = 0$ [Fig. 2(f)]. Therefore, the interaction between the emitter, the mode $\hat{a}_0$, and the selected mechanical mode will be described by the Hamiltonian in Eq. (1).

Figures 2(g)–2(h) show an implementation of this model in a photonic crystal nanobeam. Cavities are defined by local periodicity variations, which yield colocalized and dispersively coupled optical and mechanical resonances [28,29]. Placing three defect cavities along one nanobeam leads to both optical and mechanical hybridization. The intercavity separation controls the optical interaction rate J. The electric field of $\hat{a}_0$ [Fig. 2(g)] is zero in the central cavity when the mechanical mode is at rest. Figure 2(h) shows the mechanical mode that provides the required detuning on the lateral cavities, which causes $\hat{a}_0$ to acquire a finite electric field in the central cavity [Fig. 2(i)].

Full model and numerical calculations.—We now analyze the three-cavity system in detail and show that it behaves as predicted by Eq. (1). For simplicity, we consider only one of the hybridized mechanical supermodes, described by the operator $\hat{b}$, frequency Ω_M, and dispersively coupled to the lateral cavities at a rate $\pm g_0/\sqrt{2}$. This approach is justified as long as the mechanical mode coupling exceeds the mechanical dissipation [19]. In a frame rotating at ω_c, the Hamiltonian is

$$\hat{H} = -\hat{\Delta}\hat{a}_L^\dagger\hat{a}_L + \hat{\Delta}\hat{a}_R^\dagger\hat{a}_R + \Omega_M\hat{b}^\dagger\hat{b} + \frac{\omega_A - \omega_c}{2}\hat{\sigma}_z + J[\hat{a}_T^\dagger(\hat{a}_L + \hat{a}_R) + \text{H.c.}] + g(\hat{a}_T\hat{\sigma}_+ + \text{H.c.}), \quad (3)$$

where we defined $\hat{\Delta} = g_0/\sqrt{2}(\hat{b} + \hat{b}^\dagger)$. The first two terms describe the mechanically induced detuning on the lateral cavities. The second row describes optical mode coupling and the Rabi interaction between emitter and cavity T. For $J \gg \Omega_M$, we can treat $\hat{\Delta}$ quasistatically [18] and diagonalize the optical part of the Hamiltonian by introducing three optical supermodes, $\hat{a}_\pm$ and $\hat{a}_0$. Up to the first order in $\hat{\Delta}/J$ (generally applicable until very large phonon numbers [19]), we obtain an effective interaction Hamiltonian

$$\hat{H}_{\rm int} = \gamma(\hat{b} + \hat{b}^\dagger)(\hat{a}_0\hat{\sigma}_+ + \text{H.c.}) + g'[(\hat{a}_+ - \hat{a}_-)\hat{\sigma}_+ + \text{H.c.}]. \quad (4)$$

The first term of Eq. (4) shows the tripartite interaction explicitly, with $\gamma = gg_0/2J$. The last term describes a Rabi interaction between the emitter and the supermodes $\hat{a}_\pm$, with coupling rate $g' = g/\sqrt{2}$. A pure tripartite interaction can therefore be obtained for significant supermode separation ($J \gg \Omega_M$) and tripartite resonance ($\omega_A \approx \omega_c \pm \Omega_M$). Additionally, to let the emitter interact with the supermodes (and not the uncoupled modes), we require $J \gg g$. To verify that the predicted coherent emitter-phonon interaction occurs in a realistic scenario, we numerically calculate the dynamics dictated by the full Hamiltonian in Eq. (3) [19,30]. Out of the many possible systems, we consider the structure of Figs. 2(g)–2(h) made in diamond with a nitrogen vacancy (NV) center as an emitter. The simulated parameters for this system are $\{\omega_c, \Omega_M, g, g_0\} = 2\pi\{4.7 \times 10^5, 14, 20, 0.004\}$ GHz. We consider $\omega_A = \omega_c + \Omega_M$ and $J = 18g$, corresponding to single-period cavity separation [19]. The lossless evolution of the three-cavity system {shown in Fig. S(3)a of [19]} agrees perfectly with that of the MFC Hamiltonian [Fig. 1(c)] and verifies the predicted QE-phonon oscillation period $\pi/\gamma = 4.5$ μs. This confirms that for realistic choices of parameters, a purely tripartite interaction is obtained in the three-cavity system. In order to overcome losses, unavoidable in an experimental setting, the coupling rate can be enhanced by selectively pumping the supermode $\hat{a}_0$ [19]. Figure 3(a) shows the evolution of the three-cavity system [Eq. (3)], with dissipations introduced through Lindblad operators [19], using cavity decay rate $\kappa/2\pi = 3$ GHz and emitter decay rate $\Gamma/2\pi = 0.05$ GHz

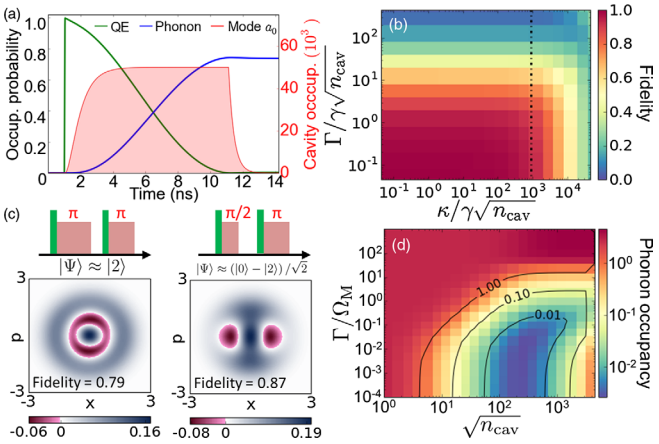

FIG. 3. Numerical calculations based on the three-cavity Hamiltonian [Eq. (3), parameters in text]. (a) The QE is excited at $T = 1$ ns and subsequently the mode $\hat{a}_0$ (red shaded area) is strongly pumped. (b) Fidelity of the created one-phonon state versus Γ and κ for $n_{\rm cav} = 5 \times 10^4$. The vertical dashed-dotted line indicates $\kappa = 2g_0J\sqrt{n_{\rm cav}}/g$. (c) Two examples of nonclassical mechanical states obtainable. Top plots: pumping sequences. Bottom plots: resultant Wigner maps of the mechanical resonator. (d) Cooling through MFC. Steady-state mean phonon number versus Γ and $n_{\rm cav}$ for continuous optical pumping and $\kappa = 10\Omega_M$.

(measured for NV centers in photonic crystals [20]). The QE is excited by a short π pulse, followed by a pulse that excites $\hat{a}_0$ to a maximum population of $n_{\rm cav} = 5 \times 10^4$, shown to be experimentally feasible in diamond [29]. We note that the emitter is not directly affected by the large optical intensity as the field is zero at its position. During the optical pulse, the mechanical mode interacts with the QE with a coupling rate $\gamma\sqrt{n_{\rm cav}}$. After a time $\Delta t = \pi/2\gamma\sqrt{n_{\rm cav}}$, the pump is switched off, suppressing the interaction and leaving the system in a one-phonon state with a fidelity of 0.86. Its nonclassical nature is emphasized by the characteristic negativity of the Wigner function (shown in Fig. S(3)b of [19]). The fidelity of the one-phonon state creation can be made arbitrarily close to one [Fig. 3(b)] by reducing the QE decay rate (so that $\Gamma \ll \gamma\sqrt{n_{\rm cav}}$) and the optical losses κ of the supermodes $\hat{a}_\pm$, which introduce additional decay for the QE due to the finite optical linewidth. This decay is negligible when $\kappa \ll 2g_0J\sqrt{n_{\rm cav}}/g$ [dashed-dotted line in Fig. 3(b)] [19]. The influence of $n_{\rm cav}$ and QE dephasing on the fidelity is discussed in the Supplemental Material [19].

The optical control of the QE-phonon interaction allows creating also other nonclassical mechanical states by pumping the QE and the optical mode with properly controlled pulse sequences. As an example, we demonstrate the preparation of a Fock state $|\Psi\rangle = |2\rangle$ and a superposition state $|\Psi\rangle = (|0\rangle - |2\rangle)/\sqrt{2}$ using the same parameters as Fig. 3(a). The QE is excited twice, each time followed by either a π- or a $\pi/2$-pulse on the optical mode. Figure 3(c) shows the resultant Wigner maps, displaying the expected nonclassical signatures for these states, which are prepared with fidelities 0.79 and 0.87, respectively. Interestingly, this interaction could also be employed to reconstruct the density matrix of mechanical states with methods analogous to trapped-ion experiments [15]. Alternative methods to characterize the produced states involve tomography using the dispersive interaction of the mechanical supermode with a different cavity mode [1].

The proposed QE-phonon interaction can also be used to cool the mechanical resonator to its ground state. The cooling cycle is triggered by a red-detuned cavity photon, which excites the QE upon annihilation of a phonon. The excitation is subsequently dissipated through the QE decay. Differently from standard optomechanical cooling [1], this mechanism can achieve ground-state cooling in the bad cavity regime ($\kappa \gg \Omega_M$), while resolved sideband operation is required only for the QE ($\Gamma < \Omega_M$). Figure 3(d) shows the steady-state phonon population in the three-cavity system versus Γ and $n_{\rm cav}$ for $\kappa = 10\Omega_M$, finite mechanical losses ($\Gamma_M/2\pi = 50$ kHz), and thermal initial phonon occupation $n_{\rm th} = 4$. As expected, ground-state cooling is possible for $\Gamma/\Omega_M \lesssim 1$. Phonon population lower than 0.1 can be achieved with $n_{\rm cav} \lesssim 10^3$ and realistic QE decay rates. The phonon population increase for large $n_{\rm cav}$ is attributed to the onset of ultrastrong coupling, as $\gamma\sqrt{n_{\rm cav}}$ approaches Ω_M. For small Γ, the QE total decay rate is dominated by the additional emission into the supermodes $\hat{a}_\pm$ (which read

$\Gamma^{(\pm)} = g^2\kappa/4J^2 \approx 2\pi \times 0.11$ GHz [19]), which explains the saturation of the phonon population for $\Gamma/\Omega_M < 10^{-2}$.

In conclusion, we have introduced a new kind of emitter-photon-phonon interaction in hybrid-optomechanical systems, based on mechanically induced variations of the electric field spatial pattern. The interaction is particularly strong in weakly interacting multicavity systems as it scales inversely with the intercavity coupling rate J. For large optical drives, this mechanism leads to an emitter-phonon coherent interaction whose strength is controlled by the optical intensity. Emitter-phonon excitation swapping and mechanical ground-state cooling are possible with feasible experimental parameters. The proposed interaction strength is much larger than effects obtainable in single-mode systems, which require the ultrastrong coupling regime ($g \approx \omega_c$) to have comparable rates [10–12,19]. Differently from strain-based methods [5–8], the proposed mechanism is not limited to a specific choice of emitters and material systems, and it could even be applied to atoms trapped near a mechanical resonator [31–33]. Moreover, it provides strong quantum nonlinearities without requiring the single-photon strong optomechanical coupling regime ($g_0 \gg \kappa$). In perspective, the proposed optically controlled emitter-phonon interaction paves the way for, e.g., control of spontaneous phonon emission, creation of nonclassical states of motion, and phonon lasing.

The authors acknowledge L. Midolo for first pointing out the possibility of displacement-induced field variations in optomechanical cavities. This work is part of the research programme of the Netherlands Organisation for Scientific Research (NWO). E. V. acknowledges an NWO-Vidi grant for financial support.

*m.cotrufo@tue.nl

[1] M. Aspelmeyer, T. J. Kippenberg, and F. Marquardt, Rev. Mod. Phys. **86**, 1391 (2014).
[2] A. D. O'Connell, M. Hofheinz, M. Ansmann, R. C. Bialczak, M. Lenander, E. Lucero, M. Neeley, D. Sank, H. Wang, M. Weides, J. Wenner, J. Martinis, and A. N. Cleland, Nature (London) **464**, 697 (2010).
[3] F. Lecocq, J. D. Teufel, J. Aumentado, and R. W. Simmonds, Nat. Phys. **11**, 635 (2015).
[4] J.-M. Pirkkalainen, S. Cho, F. Massel, J. Tuorila, T. Heikkilä, P. Hakonen, and M. Sillanpää, Nat. Commun. **6**, 6981 (2015).
[5] I. Wilson-Rae, P. Zoller, and A. Imamoglu, Phys. Rev. Lett. **92**, 075507 (2004).
[6] T. Ramos, V. Sudhir, K. Stannigel, P. Zoller, and T. J. Kippenberg, Phys. Rev. Lett. **110**, 193602 (2013).
[7] D. A. Golter, T. Oo, M. Amezcua, K. A. Stewart, and H. Wang, Phys. Rev. Lett. **116**, 143602 (2016).
[8] M. Munsch, A. V. Kuhlmann, D. Cadeddu, J.-M. Gérard, J. Claudon, M. Poggio, and R. J. Warburton, arXiv:1608.03082.
[9] J. Restrepo, C. Ciuti, and I. Favero, Phys. Rev. Lett. **112**, 013601 (2014).
[10] S. Barzanjeh, M. H. Naderi, and M. Soltanolkotabi, Phys. Rev. A **84**, 063850 (2011).
[11] Y. Chang, H. Ian, and C. Sun, J. Phys. B **42**, 215502 (2009).
[12] W. Wang, L. Wang, and H. Sun, J. Korean Phys. Soc. **57**, 704 (2010).
[13] K. A. Fisher, D. G. England, J.-P. W. MacLean, P. J. Bustard, K. J. Resch, and B. J. Sussman, Nat. Commun. **7**, 11200 (2016).
[14] K. Lee, B. Sussman, M. Sprague, P. Michelberger, K. Reim, J. Nunn, N. Langford, P. Bustard, D. Jaksch, and I. Walmsley, Nat. Photonics **6**, 41 (2012).
[15] D. Leibfried, R. Blatt, C. Monroe, and D. Wineland, Rev. Mod. Phys. **75**, 281 (2003).
[16] J. D. Joannopoulos, S. G. Johnson, J. N. Winn, and R. D. Meade, *Photonic Crystals: Molding the Flow of Light* (Princeton University Press, Princeton, NJ, 2011).
[17] T. K. Paraïso, M. Kalaee, L. Zang, H. Pfeifer, F. Marquardt, and O. Painter, Phys. Rev. X **5**, 041024 (2015).
[18] M. Ludwig, A. H. Safavi-Naeini, O. Painter, and F. Marquardt, Phys. Rev. Lett. **109**, 063601 (2012).
[19] See Supplemental Material http://link.aps.org/supplemental/10.1103/PhysRevLett.118.133603 for the derivation of Eqs. (3)–(4) and further details on the validity of the approximations involved, on the role of the other supermodes in the three-cavity system, on the generation of the nonclassical states and on the numerical simulations of the structure in Fig. 2(g)–2(h), which includes Refs. [20–25].
[20] J. C. Lee, D. O. Bracher, S. Cui, K. Ohno, C. A. McLellan, X. Zhang, P. Andrich, B. Alemán, K. J. Russell, A. P. Magyar, I. Aharonovich, A. B. Jayich, D. Awschalom, and E. L. Hu, Appl. Phys. Lett. **105**, 261101 (2014).
[21] M. A. Nielsen and I. L. Chuang, *Quantum Computation and Quantum Information* (Cambridge University Press, Cambridge, 2000), Vol. 2, pp. 23.
[22] A. Faraon, C. Santori, Z. Huang, V. M. Acosta, and R. G. Beausoleil, Phys. Rev. Lett. **109**, 033604 (2012).
[23] P. Lodahl, S. Mahmoodian, and S. Stobbe, Rev. Mod. Phys. **87**, 347 (2015).
[24] L. Robledo, H. Bernien, I. van Weperen, and R. Hanson, Phys. Rev. Lett. **105**, 177403 (2010).
[25] C. K. Law and J. H. Eberly, Phys. Rev. Lett. **76**, 1055 (1996).
[26] R. Johne, R. Schutjens, S. Fattah Poor, C.-Y. Jin, and A. Fiore, Phys. Rev. A **91**, 063807 (2015).
[27] N. Caselli, F. Riboli, F. La China, A. Gerardino, L. Li, E. H. Linfield, F. Pagliano, A. Fiore, F. Intonti, and M. Gurioli, ACS Photonics **2**, 565 (2015).
[28] J. Chan, T. M. Alegre, A. H. Safavi-Naeini, J. T. Hill, A. Krause, S. Gröblacher, M. Aspelmeyer, and O. Painter, Nature (London) **478**, 89 (2011).
[29] M. J. Burek, J. D. Cohen, S. M. Meenehan, T. Ruelle, S. Meesala, J. Rochman, H. A. Atikian, M. Markham, D. J. Twitchen, M. D. Lukin, O. Painter, and M. Lončar, Optica **3**, 1404 (2016).
[30] J. Johansson, P. Nation, and F. Nori, Comput. Phys. Commun. **183**, 1760 (2012).
[31] A. Goban, C.-L. Hung, S.-P. Yu, J. Hood, J. Muniz, J. Lee, M. Martin, A. McClung, K. Choi, D. Chang, O. Painter, and H. Kimble, Nat. Commun. **5**, 3808 (2014).
[32] J. Thompson, T. Tiecke, N. de Leon, J. Feist, A. Akimov, M. Gullans, A. Zibrov, V. Vuletić, and M. Lukin, Science **340**, 1202 (2013).
[33] K. Hammerer, M. Wallquist, C. Genes, M. Ludwig, F. Marquardt, P. Treutlein, P. Zoller, J. Ye, and H. J. Kimble, Phys. Rev. Lett. **103**, 063005 (2009).